JOC Article

Photochemical Generation of Oligodeoxynucleotide Containing a C4′-Oxidized Abasic Site and Its Efficient Amine Modification: Dependence on Structure and Microenvironment

Kazuteru Usui, Mariko Aso,* Mitsuhiro Fukuda, and Hiroshi Suemune*

Graduate School of Pharmaceutical Sciences, Kyushu University, Maidashi, Higashi-ku, Fukuoka 812-8582, Japan

aso@phar.kyushu-u.ac.jp

Received September 22, 2007

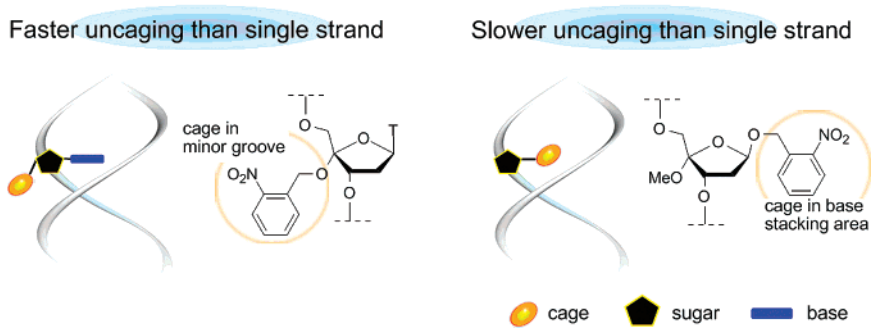

Bleomycin-induced oxidative DNA damage under limited oxygen conditions results in the formation of the C4′-oxidized abasic site (**1**). We synthesized the oligodeoxynucleotides (ODN) **5**, which contains 4′-*o*-nitrobenzyloxythymidine (**3**), and **6**, which contains 2-nitrobenzyloxy-4′-methoxy-2′-deoxy-D-ribofuranoside (**4**), as the caged precursors of **7**, an ODN containing **1**, to study its reactivity with amines. Photoirradiation of the single- and double-stranded **5** led to the formation of **7**. Uncaging of the duplex was faster and the yield of **7** was higher with the double-stranded than with the single-stranded ODN. It was suggested that a low dielectric environment of the *o*-nitrobenzyloxy group in the minor groove of the duplex might accelerate the uncaging rate. Similarly, **6** and its duplex yielded **7** by photoirradiation. However, the yields of **7** were lower than those of **5**, and duplex formation slowed the uncaging rate. Reaction of the obtained **7** with an amine resulted in the formation of the lactam **2b** in good yield in both single- and double-stranded forms, showing that amine modification of biomolecules by an ODN containing **1** is possible under physiologic conditions.

Introduction

Bleomycin-induced oxidative DNA damage under limited oxygen conditions results in the formation of the alkali-labile C4′-oxidized abasic site (**1**) via the C4′ hydrogen abstraction of 2′-deoxyribose and the subsequent oxidation of the resulting C4′ radical to the C4′ cation (Scheme 1).[1] At equilibrium, the 1,4-dihydroxytetrahydrofuran structure of **1** can exist in the open form with a 1,4-dicarbonyl structure. Reactive aldehydes, especially bifunctional ones, can be toxic as a result of their reactivity with a DNA base and a protein.[2] We found that an unsaturated lactam (**2a**) and DNA fragments were formed in the reaction of an oligodeoxynucleotide (ODN) containing **1** with an amine under mild conditions (room temperature, pH 7).[3,4] This indicates that the ODN containing **1** provides a reactive keto aldehyde moiety and possibly modifies the amine-containing biomolecules that interact with DNA. Lactam formation from ODN containing **1** proceeds without extra reagents, such as $NaBH_4$, as in the lysine modification via a Schiff base.

(1) Sugiyama, H.; Kilkuskie, R. E.; Hecht, S. M.; van der Marel, G. A.; van Boom, J. H. *J. Am. Chem. Soc.* **1985**, *107*, 7765−7767.

(2) (a)Nechev, L. V.; Harris, C. M.; Harris, T. M. *Chem. Res. Toxicol.* **2000**, *13*, 431−435. (b) Xu, G.; Liu, Y.; Kansal, M. M.; Sayer, L. M. *Chem. Res. Toxicol.* **1999**, *12*, 855−861. (c) Chen, L.-J.; Hecht, S. S.; Peterson, L. A. *Chem. Res. Toxicol.* **1997**, *10*, 866−874.

(3) Aso, M.; Kondo, M.; Suemune, H.; Hecht, S. M. *J. Am. Chem. Soc.* **1999**, *121*, 9023−9033.

(4) Aso, M.; Ryuo, K.; Kondo, M.; Suemune, H. *Chem. Pharm. Bull.* **2000**, *48*, 1384−1386.

10.1021/jo702080r CCC: $40.75
Published on Web 12/07/2007

SCHEME 1. Formation of 1 and Its Reaction with Amine Forming Lactam

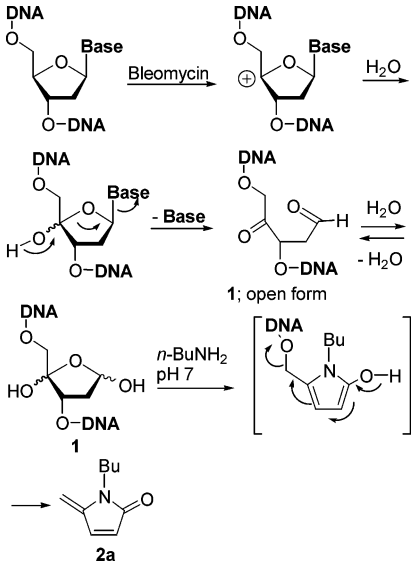

CHART 1. Caged Nucleoside 3, Caged Sugar 4, and ODNs Containing DnaA Binding Site

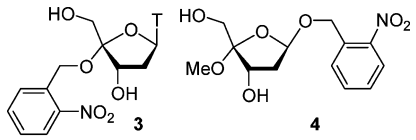

5′-$C_1C_2X_3G_4T_5G_6G_7A_8T_9A_{10}A_{11}C_{12}A_{13}$-3′

5; **X** = **3**
6; **X** = **4**
7; **X** = **1**
8; **X** = thymidine

5′-$T_1G_2T_3T_4A_5T_6C_7C_8A_9C_{10}Y_{11}G_{12}G_{13}$-3′

9; **Y** = adenosine
10; **Y** = guanosine
11; **Y** = thymidine
12; **Y** = cytidine

In situ modification and mapping of the lysine residues in the reaction of ODN containing **1** may be applicable in the structure−function studies of DNA-binding proteins.

For such studies, the efficient synthesis of **1** in ODN and quantitative studies of its lactam formation are necessary. Due to its instability, especially under alkaline conditions, we planned to synthesize ODN carrying a stable caged precursor that yields **1** by photolysis. Recently, Greenberg et al. have reported the generation of **1** by photochemical cleavage of caged sugars, which carry 3,4-dimethoxy-6-nitrobenzyloxy groups at the C1 and C4 positions of the 2′-deoxyribose.[5] The 5′-*O*-silylated *O*-methyl phosphoramidites prepared from the caged sugars were incorporated into an ODN. Greenberg et al. then studied the chemical stability and biological effects of ODN containing **1**.[5] In contrast, we designed a caged nucleoside, compound **3** (Chart 1), which retains the base moiety at the C1′position and has an *o*-nitrobenzyloxy group at the C4′position to investigate the reactivity of an ODN containing **1** with amine. We believe that the use of our caged nucleoside will be advantageous for site-specific lysine modification of a targeted protein, because irradiation of a caged ODN−protein complex was possible, in which the interaction of the retained base moiety and the target protein can be maintained. Thus, we prepared the ODN **5** containing 4′-*o*-nitrobenzyloxythymidine (**3**) (Chart 1). We also designed **6**, in which a caged sugar (**4**) is introduced, to compare its uncaging efficiency with that of **5**. Some caged precursors of DNA and RNA containing an abasic site have an *o*-nitrobenzyloxy group at the C1 position of the corresponding sugars, and their photolysis results in the formation of abasic sites containing oligonucleotide.[6] The introduction of an *o*-nitrobenzyloxy group at the C1 position of deoxyribose together with a methoxy group at the C4 position appears to be another promising design for the precursor of **1**. An *o*-nitrobenzyloxy ketal structure in **3** and an *o*-nitrobenzyloxy acetal structure in **4** may show different efficiency in the photolysis of **5** and **6**. In addition to the difference in the chemical structure, duplex formation may place the *o*-nitrobenzyloxy group of **5** and **6** into different environments, i.e., the *o*-nitrobenzyloxy group in the minor groove in **5** and that between the stacked base pairs in **6**, thus affecting their photoreactivity. The sequence of **8**, the unmodified parent ODN of **5** and **6**, contains the binding site of the DnaA protein, which is involved in the initiation of replication in *Escherichia coli* (Chart 1). Recently, the X-ray crystal structure of a complex of the DNA binding domain (domain IV) of the DnaA protein and the duplex **8** has been reported.[7] The results of X-ray crystallography suggest that one of the lysine residues in domain IV (Lys-$_{415}$) is located near the phosphate group between C2 and T3. The open form of **7** may react with Lys-$_{415}$ to modify it if the lysine residue comes near the carbonyl functions during molecular vibration of the protein conformation in solution. In this report, we describe the synthesis of **6** using conventional phosphoramidite chemistry and studies on the uncaging reactions of single- and double-stranded forms of **5** and **6**, along with the detailed kinetics. The choice of a caged monomer and the structure of ODN affected the efficiency of the uncaging reaction, and the duplex **5** yielded **7** most efficiently in this study. Subsequent amine treatment of **7** resulted in smooth lactam formation.

Results and Discussion

Synthesis of 6. The caged sugar **4** was synthesized using essentially the same methods as for the synthesis of **3**[8] via the 4,5-unsaturated **16** (Scheme 2). Koenigs−Knorr-type glycosidation of 1-chloro-3,5-di-*p*-chlorobenzoyl-D-ribofuranose[9] with *o*-nitrobenzylalcohol in the presence of AgOTf gave the desired β-anomer **13a** (28%) and α-anomer **13b** (47%). The use of $ZnCl_2$ as a catalyst increased the ratio of **13a**/**13b** to 1.3/1 (69%). Treatment of **13b** with TMSOTf in CH_3CN resulted in partial epimerization at the C1 position to give **13a**/**13b** in the ratio of 1/1.5 (68%). The stereochemistry of **13a** was determined by

(5) (a) Kim, J.; Gil, J. M.; Greenberg, M. M. *Angew. Chem., Int. Ed.* **2003**, *42*, 5882−5885. (b) Greenberg, M. M.; Weledji, Y. N.; Kroeger, K. M.; Kim, J.; Goodman, M. F. *Biochemistry* **2004**, *43*, 2656−2666. (c) Greenberg, M. M.; Weledji, Y. N.; Kim, J.; Bales, B. C. *Biochemistry* **2004**, *43*, 8178−8183. (d) Kroeger, K. M.; Kim, J.; Goodman, M. F.; Greenberg, M. M. *Biochemistry* **2004**, *43*, 13621−13629.

(6) (a) Peoc'h, D.; Meyer, A.; Imbach, J. −L.; Rayner, B. *Tetrahedron Lett.* **1991**, *32*, 207−210. (b) Trzupek, J. D.; Sheppard, T. L. *Org. Lett.* **2005**, *7*, 1493−1496.

(7) Fujikawa, N.; Kurumizaka, H.; Nureki, O.; Terada, T.; Shirouzu, M.; Katayama, T.; Yokoyama, S. *Nucleic Acids Res.* **2003**, *31* (8), 2077−2086.

(8) Aso, M.; Usui, K.; Fukuda, M.; Kakihara, Y.; Goromaru, T.; Suemune, H. *Org. Lett.* **2006**, *8*, 3183−3186.

(9) Ishido, R.; Kyomoro, H.; Nagase, T.; T katsuki, K.; Nakajima, C.; Ooshida, H. Jpn. Kokai Tokkyo Koho JP 07224081 A 19950822 Heisei, 1995.

SCHEME 2. Synthesis of Phosphoramidite 18 for ODN 6

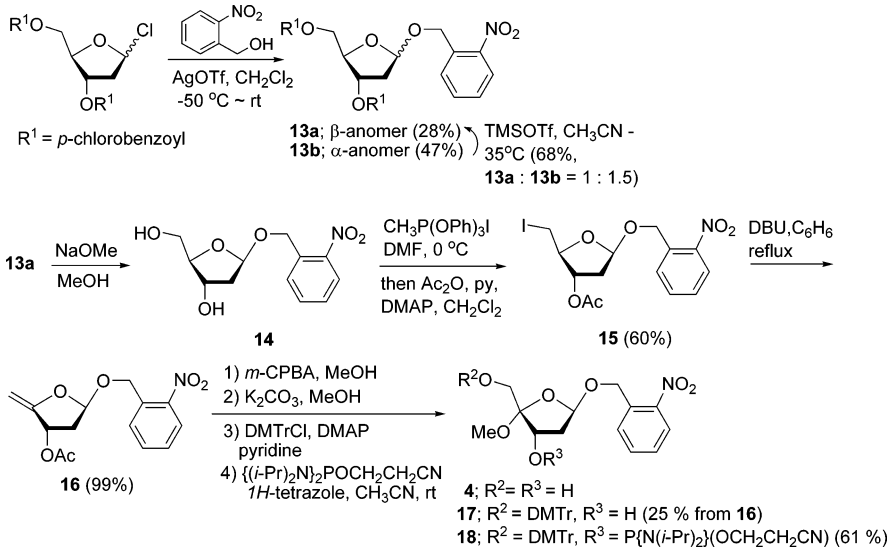

SCHEME 3. Photolysis of 5 and 6 To Give 7

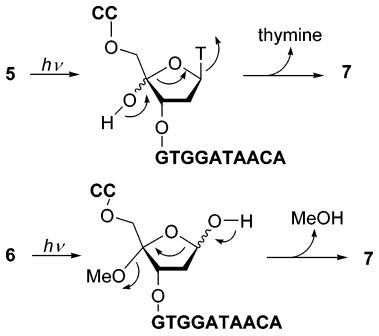

the X-ray analysis of **14**, which was further converted into the intermediate **16** via **15**. Treatment of **16** with *m*-CPBA in MeOH and subsequent solvolysis of the acetate group produced an inseparable mixture of **4** and its C4 epimer (1:1). Protection of the 5′-hydroxyl group as a DMTr ether facilitated the chromatographic separation of the diastereomers, and **17** was obtained in 25% yield from **16**. The phosphoramidite **18** prepared from **17** was incorporated into the 13-mer using the conventional phosphoramidite method with an automated DNA synthesizer. ODN synthesized in the trityl on mode was purified by HPLC, and the DMTr group of the ODN was removed under acidic conditions (15% AcOH, 0 °C, 3 h) to give **6** (Supporting Information). The structure of **6** was confirmed by MALDI-TOF MS ((*m*/*z*) 4016 (calculated for **6**: 4015)).

Photoreaction of 5. The photoreaction of **5**[8] was studied in a 10 μM solution in water or phosphate buffer (10 mM, pH 7), both containing 100 mM NaCl and **8** (3 μM), which was added to the reaction mixture as an internal standard (Scheme 3, Figure 1a). HPLC analysis of the photoirradiated **5** (retention time at 26 min) at 365 nm indicated its smooth conversion to a new product (19 min) in 30 min (the peak at 20 min is the internal standard **8**). The liberation of thymine (6 min) was also confirmed by co-injection of the reaction mixture and thymine, suggesting that the uncaging reaction occurred (Supporting Information). The peak at 19 min was assigned to **7** on the basis its conversion to the lactam as described in the last paragraph.[8] The formation of **7** was also confirmed by analysis of the MALDI-TOF MS spectrum of the photolyzed sample, which showed peaks assigned to **7** (3866; calculated for **7**: 3865), its open dehydrated form (3849; calculated for **7** − H_2O: 3847), and sodium-added form (3888; calculated for **7** + Na: 3888) (Supporting Information).

Studies of the decaging kinetics showed that the decay of **5** followed first-order kinetics in both water and phosphate buffer with comparable rate constants of $k = 1.5 \times 10^{-1}$ min^{-1} and $t_{1/2} = 4.6$ min (Figure 2a and Table 1). The yield of ODN **7** at 30 min was estimated to be about 70% based on a comparison of the peak areas of **7** and **8** (Figure 2c).[10] For preparation of the duplex containing **1**, Greenberg et al. hybridized an ODN containing **1** under mild conditions (37 °C) because of its instability at high temperature (above 55 °C).[5a] The direct formation of the duplex containing **1** by photoirradiation of the duplex caged ODN would be convenient if the reaction proceeded efficiently.

Therefore, the photoreaction of the duplex **5** was studied next. Prior to the photoreaction, UV melting studies were carried out to determine the stability of the duplex **5**. The T_m value indicated that the duplex of **5** with **9** was stable (41.5 and 46.4 °C in H_2O and phosphate buffer, respectively, Table 2, entry 5) under the photoreaction conditions employed (25 °C), although the stability was slightly less than that of the unmodified **8**:**9** (Table 2, entry 1). The duplexes of **5** with the ODN containing base other than adenine at Y (entries 6−8) were less stable than **5**:**9** (entry 5), indicating that the thymine in **3** formed a base pair with the opposite adenine in the duplex. Detmer et al. studied the impact of the C4′-alkylation of thymidine on the duplex stability.[11] The introduction of one modified thymine residue with a methyl, ethyl, and isopropyl group at the C4′ position into the duplex had little effect on its thermal stability and conformation. The duplex **5** was not destabilized significantly, and its CD spectrum was consistent with a B-type helix (Supporting Information). Interestingly, the duplexes of **5** with a mismatch were slightly more stable compared with the unmodified duplexes containing the same mismatch [Table 2, entries 6−8, $\Delta T_m'$, T_m (**8**:**10**, **11**, **12**) − T_m (**5**:**10**, **11**, **12**)]. It is known that a minor groove binder conjugated to DNA stabilizes

(10) HPLC analysis of the reaction mixture suggetsed that the peak areas of **8** and **9**, and 7-mer, 5′-**CCT**-**GTG**-**G**-3′, the internal standards, were not changed during reactions.

(11) Detmer, I.; Summerer, D.; Marx, A. *Chem. Commun.* **2002**, 2314−2315.

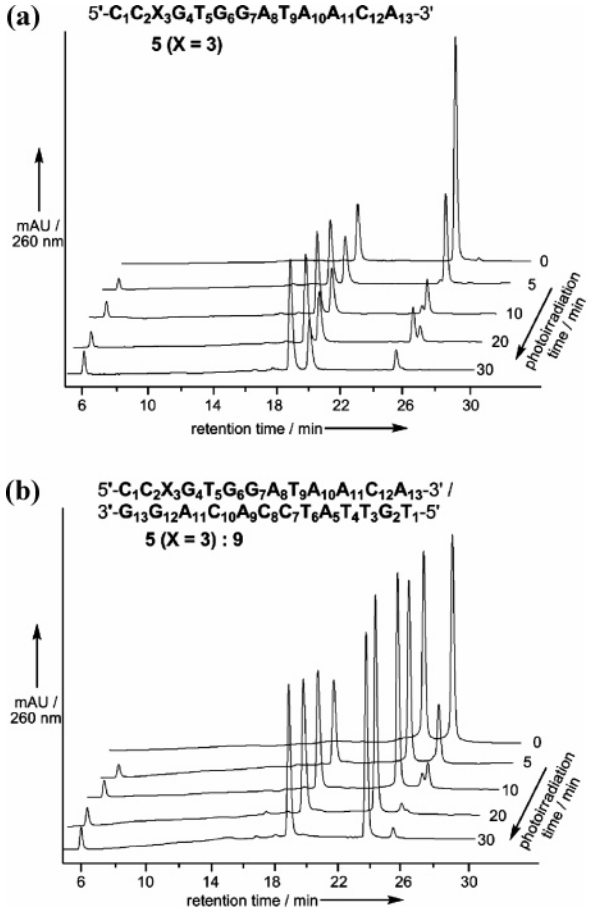

FIGURE 1. HPLC analysis of the photoirradiation of (a) **5** (retention time at 26 min, with **8** as an internal standard at 20 min) and (b) the duplex **5** (retention time at 26 min, with **9** at 24 min) at different time intervals in phosphate buffer. The ODN **7** and thymine eluted at 19 and 6 min, respectively.

duplexes, and the van der Waals interaction can be a factor in stabilizing conjugated duplexes.[12] The *o*-nitrobenzyloxy group of **3** did not make a contribution to the stabilization of the full-match duplex but to the duplex containing the mismatch. Upon irradiation in water, the duplex **5**:**9** was photolyzed by first-order kinetics with a rate constant of $k = 2.2 \times 10^{-1}$ min^{-1} and $t_{1/2}$ of 3.1 min. The decay of **5** and formation of **7** were faster in the duplex than in the single-stranded form. In phosphate buffer, the duplex **5**:**9** decayed even faster than in water with a rate constant of $k = 2.9 \times 10^{-1}$ min^{-1} and $t_{1/2} =$ 2.4 min, about 2-fold faster than the single-stranded form (Figures 1b and 2a and Table 1). The yield of **7** from the duplex **5**:**9** was also higher in both water and phosphate buffer (82% at 30 min based on the peak area of **9**[10]) than that from **5** (Figure 2c and Table 1).

Acceleration of the uncaging reaction of **5** was observed upon duplex formation. In phosphate buffer, in which the T_m value was higher than in water, the decaging reaction of the duplex was faster than in water and the more stable duplex formation resulted in a faster reaction. The *o*-nitrobenzyloxy group at the C4′ position of 2′-deoxyribose may be located in the minor groove of the duplex. We therefore focused on the microenvironment of the minor groove of the DNA duplex. It was reported that the minor groove of the B-form DNA duplex is quite nonpolar and exhibits a local dielectric constant of *ca.* 20 D, which corresponds to that of 60% 1,4-dioxane in water.[13] In order to study the effects of the dielectric environment of the minor groove on acceleration of the decaging reaction of the

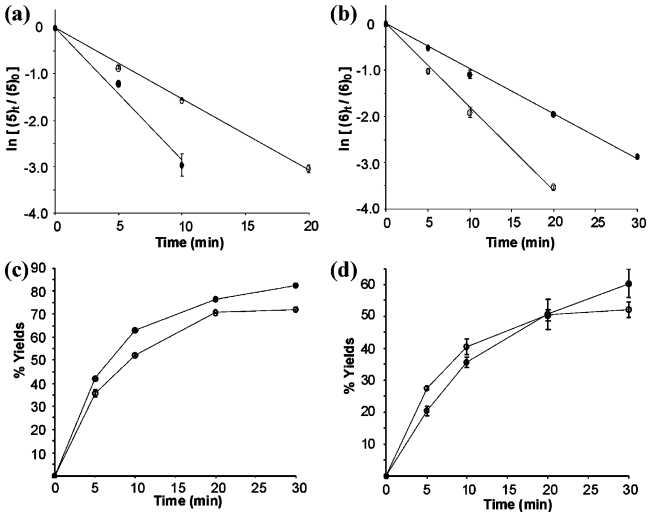

FIGURE 2. Kinetics of the decaging of (a) **5** and (b) **6** in the single-stranded (○) and duplex forms (●) in phosphate buffer. Plots of the ln substrate fractions versus time show k values of 1.5×10^{-1} and 2.9×10^{-1} min^{-1} for **5** and its duplex and 1.8×10^{-1} and 1.0×10^{-1} min^{-1} for **6** and its duplex, respectively. Yields of **7** formed by the uncaging of (c) **5** and (d) **6** in the single-stranded (○) and duplex forms (●) in phosphate buffer were calculated from peak areas of **7** based on a comparison of the corresponding internal standard.

TABLE 1. Summary of Parameters of the Photoreaction of 5 and 6 in Phosphate Buffer.

	5		**6**	
	ss[a]	ds[b]	ss[a]	ds[b]
k (min^{-1})	1.5×10^{-1}	2.9×10^{-1}	1.8×10^{-1}	1.0×10^{-1}
k_{rel}[c]	1	1.9	1.2	0.7
$t_{1/2}$ (min)	4.6	2.4	3.9	6.9
7 (%)	72 ± 1	82 ± 1	52 ± 3	60 ± 4

[a] Single stranded. [b] Double-stranded. [c] k/k_{5ss}

TABLE 2. T_m Values of Duplexes[a]

d(5′-CC**X**-GTG-GAT-AAC-A-3′)
d(3′-GG**Y**-CAC-CTA-TTG-T-5′)

		T_m, (°C)		ΔT_m (°C)[d]		$\Delta T_m'$ (°C)[e]	
entry	duplex (**X**:**Y**)	H_2O[b]	PB[c]	H_2O[b]	PB[c]	H_2O[b]	PB[c]
1	**8**:**9** (**T**:**A**)	42.4	47.7				
2	**8**:**10** (**T**:**G**)	36.8	41.7	−5.6	−6.0		
3	**8**:**11** (**T**:**T**)	34.7	39.2	−7.7	−8.5		
4	**8**:**12** (**T**:**C**)	32.6	33.2	−9.8	−14.5		
5	**5**:**9** (**3**:**A**)	41.5	46.4	−0.9	−1.3	−0.9	−1.3
6	**5**:**10** (**3**:**G**)	37.0	43.1	−5.4	−4.6	0.2	1.4
7	**5**:**11** (**3**:**T**)	35.5	41.5	−6.9	−6.2	0.8	2.3
8	**5**:**12** (**3**:**C**)	33.0	34.7	−9.4	−13.0	0.4	1.5
9	**6**:**9** (**4**:**A**)	27.0	37.7	−15.4	−10.0		

[a] Data were obtained from the average of three individual experiments. Measurements were conducted with 3 μM duplex DNA in water or buffer, both containing 0.1 M NaCl. Melting temperatures were obtained from the maximum of the first derivative of the melting curve (A_{260} vs temperature). [b] Measurements conducted in water. [c] Measurements condoucted in 10 mM phosphate buffer (pH 7). [d] $\Delta T_m = T_m - T_m$ (**8**:**9**). [e] $\Delta T_m' = T_m$ (**8**:**9**, **10**, **11**, **12**) − T_m (**5**:**9**, **10**, **11**, **12**).

(12) Kumar, S.; Reed, M. W.; Gamper, H. B., Jr.; Gorn, V. V.; Lukhtanov, E. A.; Foti, M.; West, J.; Meyer, R. B., Jr.; Schweitzer, B. I. *Nucleic Acids Res.* **1998**, *26*, 831−838.

duplex **5**, photoreaction of single-stranded **5** was conducted in 60% 1,4-dioxane in phosphate buffer. Interestingly, the uncaging reaction proceeded with efficiency comparable to that of the duplex in phosphate buffer ($k = 2.4 \times 10^{-1}$ min^{-1}, yield of **7** = 88%, Supporting Information). This result clearly indicates that a low dielectric environment in the minor groove accelerates the uncaging reaction of the duplex. Solvent dependence of the photo cleavage of the *o*-nitrobenzyl linker was reported,[14] and photolysis of the veratryl-based linker was faster in 1,4-dioxane than in aqueous solvents. The UV spectra of **3** were recorded in phosphate buffer and buffer containing 60% dioxane. The absorbance at 365 nm due to n-π* excitation did not show any difference in the two buffers (data not shown). During photolysis of the *o*-nitrobenzyl ether, the reaction rates of the *aci*-nitro intermediate is also solvent dependent,[15] and further studies are required to determine which steps in the uncaging process are affected by the dielectric environment during acceleration of the uncaging of **5**.

Photoreaction of 6. The photoreactions of both the single- and double-stranded forms of **6** were studied in phosphate buffer (Scheme 3). First, irradiation of **6** at 365 nm led to its decay (Figure 3a). After 30 min of irradiation, the peak of **6** (retention time at 40 min) completely disappeared and the main peak appeared at 29 min[16] along with several minor peaks. When the photolyzed sample was analyzed 1 h after irradiation, a small peak at 30 min disappeared and the area of the main peak increased. The peak at 30 min was possibly an intermediate of the uncaging reaction, although its structure was not identified. For this reason, the photoirradiated samples were left to stand for 60 min before analysis. MALDI-TOF MS measurement of the photolyzed **6** showed a peak at the *m*/*z* values of 3865, suggesting the formation of **7** (Supporting Information). Next, the photolyzed **6** and **5** were coinjected (Figure 3b). The main peak of the photolyzed **6** coeluted with **7** yielded by the photolysis of **5**, indicating that they are identical.

Kinetic studies of the uncaging of **6** were carried out based on HPLC analysis. The photolysis of **6** proceeded even faster than that of **5** ($k = 1.8 \times 10^{-1}$ min^{-1}, $t_{1/2} = 3.9$ min, Figure 2b and Table 1). The conversion of **6** to **7** appeared to be efficient based on the results of HPLC analysis of the reaction mixture (Figure 4a).[6] However, the yield of **7** based on a comparison of its peak area with an internal standard (7-mer, 5′-**CCT-GTG-G**-3′,[10] 19 min) was lower than expected (52%), probably due to formation of byproducts (Figure 2d and Table 1). Next, the photoreaction of the duplex **6** was examined 60 min after photoirradiation (Figure 4b). Photoreaction of the duplex **6** afforded **7** in 60% yield at 30 min (94% conversion). The CD spectrum of the duplex **6** was consistent with a B-type helix (Supporting Information), although the T_m value of **6** at 38 °C in phosphate buffer was lower when compared with that of the unmodified **8** and **5** (Table 2, entries 9, 1, and 5). Duplex formation of **6** under photoreaction conditions also increased the yield of **7** (60%, Figure 2d and Table 1). In contrast to the photoreaction of **5**, duplex formation decelerated the uncaging reaction of **6**, and the kinetic parameters indicated that the reaction was 0.6-fold slower than that of the single-stranded **6**

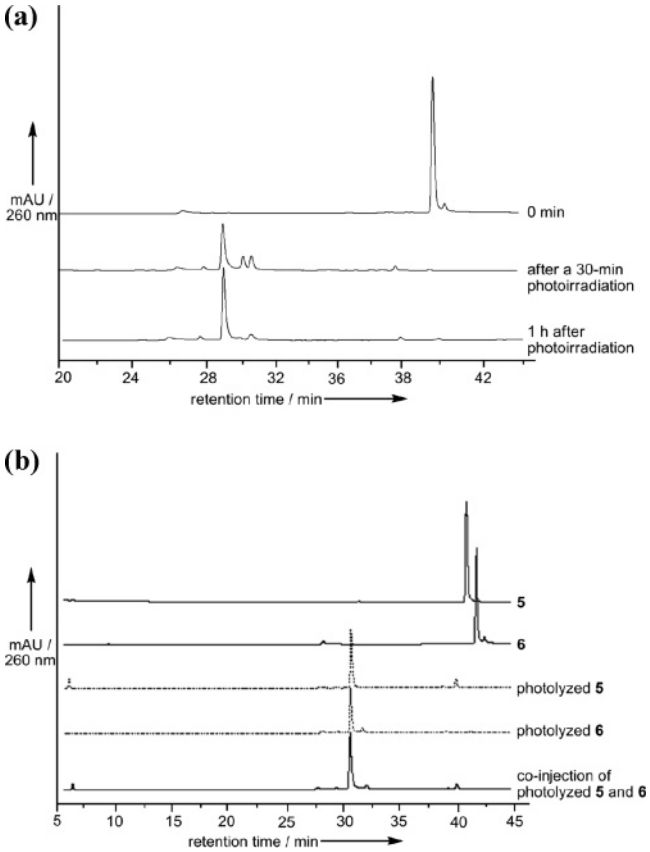

FIGURE 3. HPLC analysis after photoirradiation of **6**. (a) Analysis of **6** 1 h after 30-min irradiation. (b) Co-injection of photolyzed **5** and **6**.

($k = 1.0 \times 10^{-1}$ min^{-1}, $t_{1/2} = 6.9$ min, Figure 2b and Table 1). Thus, the formation of **7** by photoirradiation of **6** proceeded, but the yields of **7** were lower than with **5** in both the single- and double-stranded forms due to the formation of byproducts. When irradiated, the aromatic nitro group can abstract a proximal hydrogen from a saturated carbon. Kotera reported the efficient synthesis of the 2′-deoxyribonolactone lesion by photoirradiation of ODN containing the 7-nitroindole nucleoside.[17] The oxygen atom of the nitro group in 7-nitroindole is sufficiently close to abstract the H-1′ atom (2.4 Å), and the photoirradiation resulted in the generation of a C1′ radical that eventually formed 2′-deoxyribonolactone. In the caged sugar **4**, the H-1′ atom is present sufficiently close to the nitro group to be abstracted, and its abstraction may compete with that of the benzyl proton for the desired uncaging reaction and result in lower yields (Supporting Information). In the duplex, the nitrobenzyl group of **6** may be located between the stacking base pairs. Deceleration of the uncaging rate in the duplex **6** might be attributed to quenching of the photoreaction of the *o*-nitrobenzyl chromophore by the stacking base residues.

Lactam Formation from 5. Although the use of lysine appeared to be appropriate as a model for modification of lysine residues of proteins, preliminary results showed that the reaction of lysine can give a mixture of α- and ϵ-lactams under conditions similar to those in the formation of **2b**. 3-Amino-1,2-propanediol and **2b** are both water-soluble, which is appropriate for the reaction and analysis. Thus, the reaction mixture of photolyzed

(13) Jin, R.; Breslauer, K. J. *Proc. Natl. Acad. Sci. U.S.A.* **1988**, *85*, 8938−8942.
(14) Holmes, C. P. *J. Org. Chem.* **1997**, *62*, 2370−2380.
(15) Schwörer, M.; Wirz, J. *Helv. Chim. Acta* **2001**, *84*, 1441−1458.
(16) In Figures 3 and 4, the retention times of **5** and **7** were different from those in Figure 1 because the photolyzed **5** and **6** were analyzed under different HPLC conditions for better peak resolution (Experimental Section).
(17) Kotera, M.; Bourdat, A.-G.; Defrancq, E.; Lhomme, J. *J. Am. Chem. Soc.* **1998**, *120*, 11810−11811.

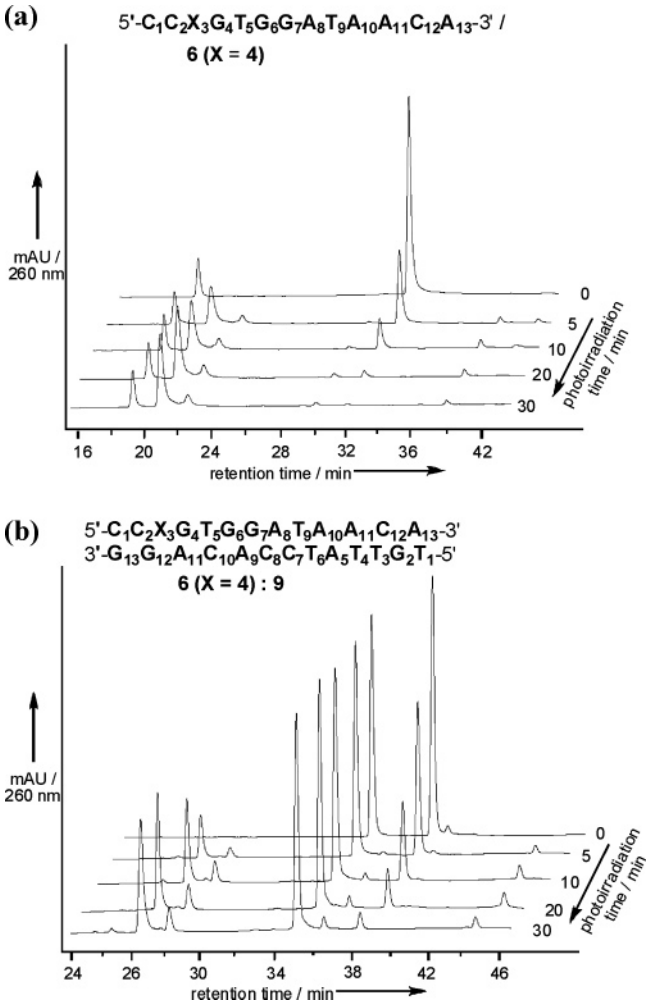

FIGURE 4. HPLC analysis of the photoirradiation of (a) **6** (retention time at 32 min, 7-mer as an internal standard and **7** eluted at 19 and 21 min, respectively) and (b) the duplex **6** (retention time at 38 min, **9** and **7** eluted at 35 and 26 min, respectively) at different time intervals. HPLC conditions are described in Experimental Section. Yields of **7** were calculated based on (a) 7-mer and (b) **9**.

SCHEME 4. Lactam Formation from 7

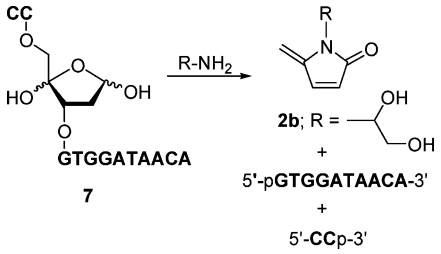

5 was subjected to a reaction with an aqueous solution of 3-amino-1,2-propanediol (1000 equiv, pH adjusted to 7 with AcOH in phosphate buffer). Heating the reaction mixture at 37 °C resulted in the conversion of **7** (18 min) to the lactam **2b** (11 min) and the fragment 10-mer (16 min) (Scheme 4 and Figure 5a; the peak at 23 min is **9**), the formations of which were confirmed by co-injection of the reaction mixture with authentic compounds and LC-MS for **2b** (Supporting Information).[8] The efficiencies of lactam formation from **7** and its duplex were comparable. The decrease in **7** followed first-order kinetics ($k = 1.5 \times 10^{-1}$ h^{-1} and $t_{1/2} = 4.6$ h for **5** and duplex **5**) (Figure 5b). The yields of lactam, determined by comparison of the peak areas with that of **9**, were virtually equal (75% and 71%, respectively, Figure 5c).

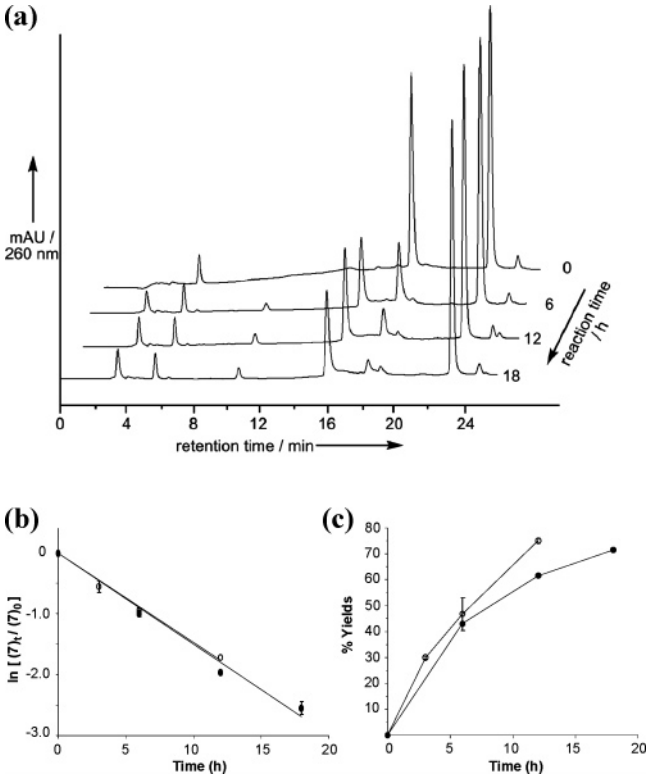

FIGURE 5. (a) HPLC analysis of the reaction mixture of the photolyzed duplex **5** and 3-amino-1,2-propanediol. The latam **2b**, the fragment 10-mer, **7**, and **9** eluted at 11, 16, 18, and 23 min, respectively. (b) Kinetics of the lactam formation from **7** in the single-stranded (○) and duplex forms (●) in phosphate buffer. Plots of ln fraction substrate present versus time give $k = 1.5 \times 10^{-1}$ h^{-1} and $t_{1/2} = 4.6$ h, respectively. (c) Yields of the lactam **2b** from **5** in the single stranded (○) and duplex forms (●) in phosphate buffer.

Conclusion

We synthesized the caged ODNs **5** and **6** using conventional phosphoramidite chemistry and studied their photocleavage reactions yielding ODN containing the C4′-oxidized abasic site (**1**). The structure and environment where a caged group was located affected the photoreactivity, and the direct photolysis of the duplex **5** enabled efficient and convenient preparation of the duplex containing **1**. Lactam formation from **7** proceeded efficiently with both the single- and double-stranded forms, indicating the possibility of protein modification using ODNs containing **1**.

Experimental Section

2-Nitrobenzyloxy-3′-5′-*O*-(di-4-chlorobenzoyl)-2′-deoxy-D-ribofuranoside (13a and 13b). Reaction with AgOTf. To a mixture of 1-chloro-3,5-di-*p*-chlorobenzoyl-D-ribofuranose (6 g, 14.1 mmol), *o*-nitrobenzyl alcohol (3.2 g, 21.1 mmol), and 3 Å molecular sieves (7 g) in dry CH_2Cl_2 (200 mL) under an Ar atmosphere was added AgOTf (10 g, 21.2 mmol) in dry THF (200 mL) dropwise during 45 min at −50 °C, and the mixture was stirred for an additional 5 h and then allowed to room temperature. After stirring for 12 h, the mixture was filtered through Celite, which was washed with CH_2Cl_2. The combined filtrates were washed with water and dried over Na_2SO_4. The solvent was evaporated and the residue was

purified by silica gel chromatography (ethyl acetate/*n*-hexane; 1:4) to give **13a** (2.2 g, 28%) and **13b** (3.6 g, 47%) as oils, respectively. **13a**: R_f = 0.39 (ethyl acetate/*n*-hexane; 1:5) × 2; ^{1}H NMR (400 MHz, $CDCl_3$) δ 8.02 (d, J = 8.2 Hz, 1H), 7.94 (m, 4H), 7.60 (m, 2H), 7.43 (m, 5H), 5.66 (m, 1H), 5.52 (m, 1H), 5.09 (d, J = 14.8 Hz, 1H), 4.92 (d, J = 14.6 Hz, 1H), 4.63−4.43 (m, 3H), 2.72−2.42 (m, 2H); HRMS-FAB (*m*/*z*) calcd for $C_{26}H_{22}Cl_2NO_8$ 546.0722 $[M + H]^+$, found 546.0737. **13b**: R_f = 0.32 (ethyl acetate/*n*-hexane; 1:5) × 2; ^{1}H NMR (400 MHz, $CDCl_3$) δ 8.07−7.30 (m, 12H), 5.48 (m, 2H), 5.22 (d, J = 14.8 Hz, 1H), 4.95 (d, J = 15.0 Hz, 1H), 4.65−4.51 (m, 3H), 2.58−2.36 (m, 2H); HRMS-FAB (*m*/*z*) calcd for $C_{26}H_{21}Cl_2NNaO_8$ 568.0542 $[M + Na]^+$, found 568.0565.

Reaction with $ZnCl_2$. To a mixture of 1-chloro-3,5-di-*p*-chlorobenzoyl-D-ribofuranose (0.5 g, 1.16 mmol), 2-nitrobenzyl alcohol (0.27 g, 1.76 mmol), $NaHCO_3$ (0.13 g, 1.55 mmol), and 4 Å molecular sieves (0.5 g) in dry CH_2Cl_2 (15 mL) was added a solution of 1 M $ZnCl_2$−Et_2O (1.8 mL) at −50 °C under an Ar atmosphere, and the mixture was stirred overnight at −50 °C. The reaction mixture was diluted with CH_2Cl_2, and the mixture was washed with saturated aqueous $NaHCO_3$ solution and brine and dried over Na_2SO_4. The solvent was evaporated under reduced pressure, and the residue was purified by silica gel chromatography (ethyl acetate/*n*-hexane; 1:4) to give **13a**/**13b**, 1.3:1 (69%). **Epimerization of 13b**. To a cooled (−35 °C) solution of **13b** (100 mg, 0.18 mmol) in CH_3CN (2 mL) was added TMSOTf (49 μL, 0.27 mmol) under an Ar atmosphere, and the mixture was stirred overnight at −35 °C. After the reaction was quenched with saturated aqueous $NaHCO_3$ solution, the mixture was evaporated. The solvent was evaporated under reduced pressure, and the residue was purified by silica gel chromatography (ethyl acetate/*n*-hexane; 1:4) to give **13a**/**13b**, 1:1.5 (68%).

2-Nitrobenzyloxy-2′-deoxy-D-ribofuranoside (14). To a suspension of **13a** (3.4 g, 6.2 mmol) in MeOH (70 mL) was added dropwise a solution of NaOMe (10 mL of a 1.85 M solution in MeOH, 18.5 mmol) at room temperature, and the mixture was stirred 3 h. After the reaction was quenched with solid NH_4Cl (2 g), the mixture was evaporated. The residue was diluted with AcOEt, washed with water, and dried over Na_2SO_4. The solvent was evaporated, and the residue was purified by silica gel chromatography (ethyl acetate/*n*-hexane; 3:1) to give **14** (1.7 g, quant): ^{1}H NMR (400 MHz, $CDCl_3$) δ 8.06 (d, J = 8.2 Hz, 1H), 7.65 (m, 2H), 7.46 (t, J = 7.7 Hz, 1H), 5.38 (d, J = 5.4 Hz, 1H), 5.14 (d, J = 14.8 Hz, 1H), 4.92 (d, J = 14.4 Hz, 1H), 4.58 (m, 1H), 4.09 (m, 1H), 3.70 (m, 2H), 2.43−2.17 (m, 3H). The structure of **14** was determined by X-ray crystallography (Supporting Information).

2-Nitrobenzyloxy-3′-*O*-acetyl-5′-iodo-2′-deoxy-D-ribofuranoside (15). To a cooled (0 °C) solution of **14** (0.98 g, 3.6 mmol) in DMF (20 mL), under an Ar atmosphere, was added dropwise over 5 min a solution of $CH_3P(OPh)_3I$ (4.4 mmol in 10 mL DMF), and the mixture was stirred for an additional 4 h. After addition of saturated aqueous $Na_2S_2O_3$ solution, the reaction mixture was extracted with Et_2O. The organic layer was washed with water and brine, dried over Na_2SO_4, and concentrated under reduced pressure. The residue was purified by silica gel chromatography (ethyl acetate/*n*-hexane; 1:4 to 1:1) to give crude product (1.5 g). Next, a mixture of the obtained crude product (1.5 g), dry pyridine (0.4 mL, 5.5 mmol), DMAP (40 mg, 0.3 mmol), and acetic anhydride (0.52 mL, 5.5 mmol) in CH_2Cl_2 (10 mL) was stirred at room temperature for 1 h. After addition of water, the reaction mixture was extracted with CH_2Cl_2. The organic layer was washed with saturated aqueous $NaHCO_3$ solution, dried over Na_2SO_4, and concentrated under reduced pressure. The residue was purified by silica gel column chromatography (ethyl acetate/*n*-hexane; 1:3) to give **15** (0.92 g, 60%): ^{1}H NMR (400 MHz, $CDCl_3$) δ 8.05 (d, J = 8.1 Hz, 1H), 7.67 (m, 2H), 7.46 (m, 1H), 5.42 (dd, J = 5.4, 2.0 Hz, 1H), 5.28 (m, 1H), 5.18 (d, J = 14.7 Hz, 1H), 4.94 (d, J = 14.7 Hz, 1H), 4.31−4.26 (m, 1H), 3.33 (m, 2H), 2.57 (m, 1H), 2.26 (m, 1H), 2.08 (s, 3H); HRMS-FAB (*m*/*z*) calcd for $C_{14}H_{17}INO_6$ 422.0101 $[M + H]^+$, found 422.0118.

2-Nitrobenzyloxy-3′-*O*-acetyl-4′,5′-methylene-2′-deoxy-D-ribofuranoside (16). Compound **15** (0.92 g, 2.2 mmol) was heated with DBU (0.97 mL, 6.5 mmol) in benzene under reflux for 5 h. After the reaction was quenched with saturated aqueous NH_4Cl solution, the mixture was evaporated. The residue was diluted with ethyl acetate and washed with water and dried over Na_2SO_4. The solvent was evaporated and the residue was purified by silica gel chromatography (CH_2Cl_2/*n*-hexane; 1:1) to give **16** (0.62 g, 97%): ^{1}H NMR (400 MHz, $CDCl_3$) δ 8.10 (d, J = 8.1 Hz, 1H), 7.73 (d, J = 7.8 Hz, 1H), 7.65 (t, J = 7.6 Hz, 1H), 7.46 (m, 1H), 5.80 (m, 1H), 5.55 (m, 1H), 5.16 (d, J = 14.9 Hz, 1H), 5.02 (d, J = 14.9 Hz, 1H), 4.50 (s, 1H), 4.25 (s, 1H), 2.53 (m, 1H), 2.22 (m, 1H), 2.09−2.11 (m, 3H); HRMS-FAB (*m*/*z*) calcd for $C_{14}H_{16}NO_6$ 294.0978 $[M + H]^+$, found 294.0959.

2-Nitrobenzyloxy-4′-methoxy-5′-*O*-(4,4′-dimethoxytrityl)-2′-deoxy-D-ribofuranoside (17) and C-4 Epimer of 17. To a solution of **16** (2.6 g, 8.9 mmol) in dry MeOH (195 mL) under an Ar atmosphere, was added dropwise a solution of *m*-CPBA (77%, 10 g, 44.6 mmol) in 72 mL of CH_2Cl_2 (predried with $MgSO_4$) over 100 min. The reaction was stirred until consumption of the substrate observed by TLC control (24 h). After addition of saturated aqueous $NaHCO_3$ solution until the pH has a value of 7, K_2CO_3 (3.7 g, 26.8 mmol) was added, and the mixture was stirred for 3 h. The reaction mixture was concentrated under reduced pressure. The residue was dissolved in AcOEt, washed with water, and dried over Na_2SO_4. The solvent was evaporated and the residue was purified by silica gel chromatography (ethyl acetate/*n*-hexane; 1:1 to ethyl acetate) to give an inseparable mixture of **4** and its epimer (1.33 g). Next, a mixture of the obtained products (0.25 g, 0.82 mmol) was coevaporated with anhydrous pyridine (twice) and dissolved in dry pyridine (6.6 mL). DMTrCl (0.36 g, 1.07 mmol) was added and the mixture was stirred overnight. The reaction mixture was cooled to 0 °C, quenched by addition of water. The resulting solution was extracted with ethyl acetate. The organic layer was washed with water and brine, dried over Na_2SO_4, and concentrated under reduced pressure. The residue was purified by silica gel chromatography (ethyl acetate/*n*-hexane; 1:3 to 1:2) to give **17** (0.25 g, 25%) and C-4 epimer of **17** (0.25 g, 25%), respectively. **17**: ^{1}H NMR (400 MHz, $CDCl_3$) δ 8.03 (dd, J = 8.1, 1.0 Hz, 1H), 7.67 (d, J = 7.8 Hz, 1H), 7.54 (td, J = 7.6, 1.0 Hz, 1H), 7.43−7.16 (m, 10H), 6.76 (m, 4H), 5.28 (d, J = 5.1 Hz, 1H), 5.10 (d, J = 15.1 Hz, 1H), 4.89 (d, J = 15.1 Hz, 1H), 4.67 (dd, J= 9.4, 7.2 Hz, 1H), 3.76 (s, 6H), 3.23−3.21 (m, 5H), 2.37 (m, 1H), 2.13 (m, 1H); HRMS-FAB (*m*/*z*) calcd for $C_{34}H_{35}NO_9$ 601.2312 $[M]^+$, found 601.2335. C-4 epimer of **17**: ^{1}H NMR (400 MHz, $CDCl_3$): δ 8.04 (d, J = 7.6 Hz, 1H), 7.78 (d, J = 7.8 Hz, 1H), 7.61 (t, J = 7.3 Hz, 1H), 7.53−7.19 (m, 11H), 6.84 (m, 4H), 5.49 (t, J = 5.4 Hz, 1H), 5.16 (d, J = 15.4 Hz, 1H), 4.94 (d, J = 15.1 Hz, 1H), 4.51 (d, J = 4.6 Hz, 1H), 3.76 (s, 6H), 3.58 (d, J = 10.0 Hz, 1H), 3.18, (s, 3H), 3.09 (d, J = 10.0 Hz, 1H) 2.43 (m, 1H), 2.25 (m, 1H); HRMS-FAB (*m*/*z*) calcd for $C_{34}H_{35}NO_9$ 601.2312 $[M]^+$, found 601.2286.

2-Nitrobenzyloxy-3′-*O*-(2-cyanoethyl *N*,*N*-diisopropylphosphoramisyl)-4′-methoxy-5′-*O*-(4,4′-dimethoxytrityl)-2′-deoxy-D-ribofuranoside (18). Compound **17** (550 mg, 0.91 mmol) was coevaporated with dry THF (3 times) and dissolved in dry CH_2Cl_2 (5 mL). 2-cyanoethyl *N*, *N*, *N*′, *N*′-tetraisopropylphosphorodiamidite (0.76 mL, 2.39 mmol) was then added under an Ar atmosphere. To the stirred solution was added dropwise a 0.9 M solution of 1*H*-tetrazole in CH_3CN (1.2 mL, 1.09 mmol), and the mixture was stirred 3 h at room temperature. The reaction mixture was diluted with CH_2Cl_2 and the mixture was washed with saturated aqueous $NaHCO_3$ solution, brine and dried over Na_2SO_4. The solvent was evaporated under reduced pressure and the residue was purified by silica gel chromatography. Elution with ethyl acetate/*n*-hexane/NEt_3; 23.5:73.5:3 to give **18** (580 mg, 79%): ^{1}H NMR (400 MHz, $CDCl_3$) δ 8.02 (d, J = 8.1 Hz, 1H), 7.72 (dd, J = 17.6, 7.7 Hz, 1H), 7.52 (dd, J = 17.5, 8.1 Hz, 1H), 7.41 (m, 3H), 7.31 (m, 4H),

7.16 (m, 3H), 6.73 (m, 4H), 5.44 (dd, J = 18.2, 5.2 Hz, 1H), 5.26 (m, 1H), 5.05 (d, 2H), 3.76 (s, 3H), 3.74 (s, 3H), 3.72−3.50 (m, 4H), 3.42 (dd, J = 15.0, 9.7 Hz, 1H), 3.27 (s, 3H), 3.02 (m, 1H), 2.62 (m, 1H), 2.54−2.31 (m, 3H), 1.17 (m, 12H); HRMS-FAB (m/z) calcd for $C_{43}H_{53}N_3O_{10}P$ 802.3469 $[M + H]^+$, found 802.3439.

Oligonucleotide Synthesis. The ODN **6** was synthesized using standard solid-phase cyanoethyl phosphoramidite chemistry on a DNA synthesizer. The oligomers were purified in DMT-on state by HPLC on a reverse-phase COSMOSIL 5C_{18}-AR-II column (20 mm i.d. × 250 mm) with a linear gradient of acetonitrile (5−40% in 40 min) in 0.1 M triethylammonium acetate (pH 7). Purified oligonucleotides were then detritylated by treatment with a solution of 15% AcOH at 0 °C for 3 h to give **6**. HPLC trace of detritylation and MALDI-TOF MS spectrum of **6** are in Supporting Information.

UV-Melting Curve Measurements. The ODN **5**, **6**, or **8** was hybridized with a 1:1 ratio (3 μM each) of **9** by heating in H_2O or 10 mM phosphate buffer (pH 7), both containing 100 mM NaCl at 80 °C for 5 min and allowed to cool to room temperature slowly, then cooled at 0 °C. Melting studies were carried out in 1 cm path length quartz cells (under nitrogen atmosphere when temperature was below 20 °C) on a UV-VISIBLE spectrometer equipped with a thermoprogrammer and temperature controller. Absorbance was monitored at 260 nm while temperature was changed at a rate of 0.5 °C min^{-1} from 0 to 80 °C. Melting temperatures were obtained from the maximum of the first derivative of the melting curve versus temperature. Hybridization of **5** and **6** with **10**, **11**, and **12** and T_m measurements were carried out similarly.

Circular Dichroism (CD) Measurements. The circular dichroism spectra were measured with a 0.1 cm path length quartz cell using a spectropolarimeter between 340 and 220 nm in 10 mM phosphate buffer (pH 7) containing 100 mM NaCl. DNA duplexes were at 3 μM. Spectra were acquired every 1 nm with a bandwidth setting of 1 nm at a speed of 50 nm min^{-1}, averaging 10 scans. CD spectra of the duplexes of **5**:**9** and **6**:**9** are in Supporting Information.

Irradiation of Single- and Double-Stranded 5. Solutions of **5** (10 μM, containing **7** (3 μM)) as an internal standard and double-stranded **5** (10 μM) were prepared in H_2O (containing 100 mM NaCl) or phosphate buffer (10 mM, pH 7, containing 100 mM NaCl) and were purged with Ar (30 min). Aliquots of these solutions (40 μL) were irradiated for 5, 10, 20, and 30 min, respectively, in a quartz cuvette with a UV lamp (λ_{max} = 365 nm, intensity 2.5 mW cm^{-2} at 364 nm) and were immediately analyzed by HPLC using a COSMOSIL 5C_{18}-AR-300 column (4.6 mm i.d. × 250 mm). Solvent A: CH_3CN. Solvent B: 50 mM ammonium formate (pH 8). Gradient: initial, 96% B for 7 min, then linear to 14% A at 35 min. Detection was carried out at 260 nm. The yields of **7** were the average of two experiments and determined by comparison of its peak area with that of **8** or **9** based on their extinction coefficients (10^5 M^{-1} cm^{-1}): **7**, 1.22; **8**, 1.30; **9**, 1.24. HPLC analysis of the reaction mixture suggested that the peak areas of **8** and **9** were not changed during the reactions. MALDI-TOF MS spectrum of the photolyzed **5** is in Supporting Information.

Irradiation of Single-Stranded 5 in 60% 1,4-Dioxane. Solutions of **5** (10 μM, containing **5-nat** (3 μM)) as an internal standard were prepared in 60% 1,4-dioxane in 10 mM phosphate buffer (pH 7) containing 100 mM NaCl and were purged with Ar (30 min). Aliquots of these solutions (40 μL) were irradiated for 5, 10, and 20 min, respectively, in a quartz cuvette with a UV lamp (λ_{max} = 365 nm, intensity 2.5 mW cm^{-2} at 364 nm) and were evaporated with a speedvac; the residues were dissolved in water (40 μL). A volume of 10 μL of the sample was immediately analyzed by HPLC similarly to the reactions in phosphate buffer. HPLC analysis of the reaction mixture is in Supporting Information.

Irradiation of Single- and Double-Stranded 6. Solutions of **6** (10 μM, containing 7-mer, 5′-**CCT-GTG-G**-3′ (3μM), as an internal standard and the double stranded **6** (10 μM) were prepared in phosphate buffer (10 mM, pH 7, containing 100 mM NaCl) and were purged with Ar (30 min). Aliquots of these solutions (40 μM) were irradiated for 5, 10, 20, and 30 min, respectively, in a quartz cuvette with a UV lamp (λ_{max} = 365 nm, intensity 2.5 mW cm^{-2} at 364 nm) and were analyzed by HPLC using a Waters XBridge C_{18} 3.5 mm column (4.6 mm i.d. × 150 mm) for single stranded **6** and a COSMOSIL 5C_{18}-AR-300 column (4.6 mm I.D. × 250 mm) for the duplex **6**. Solvent A: CH_3CN. Solvent B: 50 mM ammonium formate (pH 7.5−8). Gradient: initial, 96% B for 10 min, then linear to 10% A at 40 min. Detection was carried out at 260 nm. The yields of **7** were the average of two experiments and determined by comparison of its peak area with that of 7-mer or **9** based on their extinction coefficients (10^5 $M^{-1}cm^{-1}$): 7-mer, 0.60. MALDI-TOF MS spectrum of the photolyzed **6** is in Supporting Information.

Acknowledgment. We thank Prof. Tsuyoshi Goromaru and Ms. Yoshie Kakihara, Fukuyama University, for LC-MS measurement. K.U. acknowledges support from JSPS research fellowship.

Supporting Information Available: ^1H NMR spectra of the compounds **13a**, **13b**, **14**, **15**, **16**, **17**, and **18**, $^1H-^1H$ COSY and $^1H-^1H$ NOESY spectra of **17**, X-ray crystallographic data of **14** in CIF format, HPLC analyses of detrytilation of caged-ODN to form **6**, co-injection of the photolyzed **5** and thymine; irradiation of **5** in 60% 1,4-dioxane, co-injection of the reaction mixture of photolyzed **5** and 3-amino-1,2-propanediol with **2b** and 10-mer, MALDI-TOF MS of **6**, photolyzed **5**, and photolyzed **6**, LC-MS of the reaction mixture of photoirradiation of **5** followed by treatment with 3-amino-1,2-propanediol and authentic **2b**, circular dichroism (CD) measurements, and ab initio calculation of **4**. This material is available free of charge via the Internet at http://pubs.acs.org.

JO702080R